

Article

A Novel Coding Metasurface for Wireless Power Transfer Applications

Nguyen Minh Tran , Muhammad Miftahul Amri , Je Hyeon Park, Sa Il Hwang, Dong In Kim 
and Kae Won Choi *

Department of Electronic, Electrical and Computer Engineering, Sungkyunkwan University (SKKU),
Suwon 16419, Korea; nmtran@skku.edu (N.M.T.); miftahulamri@g.skku.edu (M.M.A.);
pjw8251@skku.edu (J.H.P.); fortyone@skku.edu (S.I.H.); dikim@skku.ac.kr (D.I.K.)

* Correspondence: kaewonchoi@skku.edu

Received: 18 October 2019; Accepted: 22 November 2019; Published: 25 November 2019



Abstract: We propose and implement a novel 1-bit coding metasurface that is capable of focusing and steering beam for enhancing power transfer efficiency of the electromagnetic (EM) wave-based wireless power transfer systems. The proposed metasurface comprises 16×16 unit cells which are designed with a fractal structure and the operating frequency of 5.8 GHz. One PIN diode is incorporated within each unit cell and enables two states with 180° phase change of the reflected signal at the unit cell. The two states of the unit cell correspond to the ON and OFF states of the PIN diode or “0” and “1” coding in the metasurface. By appropriately handling the ON/OFF states of the coding metasurface, we can control the reflected EM wave impinged on the metasurface. To verify the working ability of the coding metasurface, a prototype metasurface with a control board has been fabricated and measured. The results showed that the coding metasurface is capable of focusing beam to desired direction. For practical scenarios, we propose an adaptive optimal phase control scheme for focusing the beam to a mobile target. Furthermore, we prove that the proposed adaptive optimal phase control scheme outperforms the random phase control and beam synthesis schemes.

Keywords: 1-bit unit cell; coding metasurface; adaptive beam focusing; wireless power transfer

1. Introduction

In the last decade, due to the increasing number of wireless and mobile devices being used, charging these devices has become a crucial problem, which is now capturing massive attention. The traditional charging method with cords is not preferable for futuristic systems and devices (e.g., Internet of Things, wireless sensor networks (WSN)). Wireless power transfer (WPT), allowing us to charge a device without any wire, is emerging as a promising technology for resolving the battery charging problem.

Since the first demonstration of WPT by Tesla in early 1900, engineers and researchers have recently come up with various techniques to transfer power wirelessly [1–3]. Among them, electrical methods, consisting of inductive coupling, magnetic resonant coupling, and electromagnetic (EM) radiation, are pervasive. While the first two methods are able to provide high transmission efficiency within a short range, EM radiation is capable of providing long-range WPT but with low efficiency [2]. Achieving both long range and high efficiency is still the main challenge in WPT which requires optimal solutions. For the case of EM radiation, beam forming and focusing is a potential solution for both long distance and high efficiency, which is enabled using phased-array antennas (PAA).

Recently, a novel concept of coding and digital metasurface has emerged as a promising and alternative technique that can perform beam focusing, multibeam, or scattering [4,5]. A metasurface consists of hundreds to thousands of unit cells which have different reflection responses to incident

EM waves. In contrast to PAA, which depends on power-hungry and active components, coding metasurface enables beam synthesis by just turning ON or OFF the PIN diode integrated with each unit cell in the metasurface. By doing that, we can actually control the reflected signal outgoing from the metasurface.

The term coding metasurface was first coined by Cui and colleagues in 2014 [4]. Since then, several works and progress have been made in this area [5–7]. Different designs of 1-bit unit cell and metasurface have been proposed in [8–13]. Yang and colleagues proposed a simple rectangular element but working effectively in metasurface. The authors first designed and fabricated 10×10 array to demonstrate the working ability of the unit cell and metasurface [8,9]. Afterwards, this work was extended to 1600 element metasurface [10–12]. In these papers, the authors theoretically and experimentally demonstrated that the 1-bit metasurface is capable of digital beam focusing, multibeam focusing, scattering, and broadside beam synthesis. A 1-bit digital reconfigurable reflective metasurface with 20×20 cells is presented for beam-scanning in [13]. In that work, the authors used a varactor diode instead of a PIN diode for achieving wider bandwidth. Some works have also focused on designing 2-bit metasurface [14,15]. For instance, a dynamic beam manipulation based on 2-bit digitally controlled coding metasurface was proposed in [14] by Huang and colleagues. To enable a 2-bit operation, the authors used two PIN diodes in each meta-atom to produce four phase responses of 0 , $\pi/2$, π , and $3\pi/2$, which correspond to four basic digital elements “00”, “01”, “10”, and “11”. Experiments and measurements were conducted, which demonstrate one-beam deflection, two- and four-beam splitting, and beam diffusion by real-time control of the bias voltage. Another work is a transmission-type 2-bit programmable metasurface for single-sensor and single-frequency microwave imaging in [15]. The authors designed the unit-cell with two layers, in which each layer contains a switchable diode for providing 2-bit control ability. Recently, there has been an increasing number of research works which focus on using metasurface in wireless power transfer [16–22]. Nevertheless, these works are just able to do fixed focusing and are definitely inapplicable for mobile devices.

For an adaptive beam focusing, the channel between each unit cell of the metasurface and the receiver should be estimated. The authors in [23–25] theoretically analyzed and proposed the method for estimating the channel in intelligent surface or programmable metasurface. The method enables channel estimation by setting a single unit cell in “ON” state and the others in “OFF” state in a training time. However, this method might be impractical, especially when it comes to huge number of unit cells in the metasurface, as the reflected signal from one unit cell is too feeble compared to the rest.

In this paper, we propose a novel 1-bit coding metasurface that can dynamically perform beam focusing to the desired direction for WPT applications. Indeed, the proposed metasurface consists of 16×16 unit cells which are designed to operate at 5.8 GHz with two states (ON/OFF states) corresponding to a 0° or 180° phase shift of the reflected signal. To obtain the unit cell for a real metasurface, we applied the fractal structure in designing the unit cell. Therefore, the unit cell has compact size with dimensions of $11 \times 11 \times 1.52 \text{ mm}^3$. In order to electrically steer the beam, appropriate ON/OFF states of the unit cells in the metasurface should be set by a control board. The beam-focusing ability of the proposed coding metasurface has been validated by the experiment. The experimental results showed that the metasurface can steer and focus the beam within the range of $(60^\circ, 0^\circ)$ in the elevation angle. For practical scenarios, an optimal phase control scheme is proposed and applied to adaptively track the mobile devices. The experimental results showed that the optimal phase control scheme performs better than the random phase control and beam synthesis schemes.

2. Coding Metasurface Theory

In contrast to the existing metasurfaces that change the design structure of each unit cell to acquire the desired reflective phase shift, the coding and digital metasurface manipulates and reflects the impinged EM wave via different states of identical unit cells with the help of PIN diodes. For the theoretical analysis, we considered a coding metasurface with $M \times N$ 1-bit unit cells as shown in Figure 1. Specifically, as incident with an EM wave, the unit cell can operate in two states with the

same reflected magnitude but 180° phase change. There are possibly two types of illuminating sources (plane wave and a point source) to be considered.

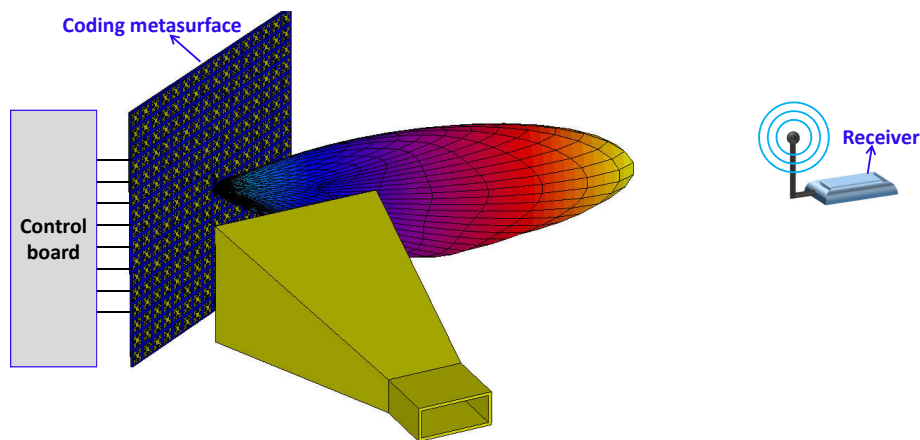


Figure 1. The coding metasurface model.

With x- or y-polarized EM wave incidence, the scattering field from the coding metasurface can be theoretically expressed as [12]

$$E(\theta, \varphi) = \sum_{m=0}^{M-1} \sum_{n=0}^{N-1} A_{mn} e^{j\alpha_{mn}} \cdot \Gamma_{mn} e^{j\phi_{mn}} \cdot f_{mn}(\theta, \varphi) \cdot e^{jk_0(md_x \sin \theta \cos \varphi + nd_y \sin \theta \cos \varphi)}, \quad (1)$$

where A_{mn} , α_{mn} are the relative illuminating amplitude and phase with respect to each unit cell in the metasurface ($A_{mn} = 1$, $\alpha_{mn} = 0^\circ$ if the source is plane wave), Γ_{mn} , ϕ_{mn} are the reflection amplitude and phase of m nth unit cell, $f_{mn}(\theta, \varphi)$ is the scattering pattern of the unit cell, and d_x and d_y indicate the unit cell spacing in x and y directions.

According to Equation (1), the scattering EM wave from the metasurface can be controlled and formed by adjusting the reflection amplitude (Γ_{mn}) and phase (ϕ_{mn}) of each unit cell. Therefore, we can say that the metasurface may possibly be encoded via these two parameters. Assuming that the reflection magnitude is identical, the reflection phase matrix with respect to the coding metasurface can be described by:

$$\Phi = \begin{bmatrix} \phi_{11} & \phi_{12} & \cdots & \phi_{1n} \\ \phi_{21} & \phi_{22} & \cdots & \phi_{2n} \\ \vdots & \vdots & \ddots & \vdots \\ \phi_{m1} & \phi_{m2} & \cdots & \phi_{mn} \end{bmatrix}_{M \times N}. \quad (2)$$

One should obtain the appropriate Φ matrix for a specific beam pattern synthesis. To focus the beam to the desired direction, the phase compensation of each unit cell can be calculated by [21]:

$$\phi_{mn} = k(|\mathbf{f} - \mathbf{r}_{mn}| + |\mathbf{d} - \mathbf{r}_{mn}|), \quad (3)$$

where k is the wavenumber, \mathbf{f} is the location of the EM source, \mathbf{d} is the location of the focusing point, and \mathbf{r}_{mn} is the position of the m nth unit cell.

2.1. Phase Quantization

The above computed phase is the ideal phase shift of each unit cell. However, only a limited phase shift can actually be provided with the coding unit cell. Hence, it is inevitable that we have to consider the phase quantization for the coding metasurface [13]. One can realize from Equation (3) that the phase compensation might be not within the range between 0 and 2π . Then, it should be shifted to

be in the range of $[0, 2\pi]$ before being quantized. Considering 1-bit coding unit cell, the shifted and quantized phase can be given as:

$$\phi_{mn}^- = \phi_{mn} - 2\pi \left[\frac{\phi_{mn}}{2\pi} \right], \quad (4)$$

$$\hat{\phi}_{mn} = \begin{cases} \pi & \text{if } \pi/2 \leq \phi_{mn}^- \leq 3\pi/2 \\ 0 & \text{elsewhere.} \end{cases} \quad (5)$$

After quantization, the reflection phase of the unit cell has just two states: 0° or 180° , corresponding to the coding “1” and coding “0”, respectively. To demonstrate the focusing ability of the coding metasurface, we computed the ideal phase and quantized phase distribution of the 16×16 coding metasurface using the above phase compensation method and the corresponding beam pattern as presented in Figure 2. The metasurface is assumed to be placed in XOY plane and is excited by a point source. Although the relative power generated by the ideal phase distribution (245) is much higher compared to one of the quantized phase distribution (around 170), both cases are capable of performing good beam steering. It is clear that beam synthesis can be acquired by 1-bit coding metasurface.

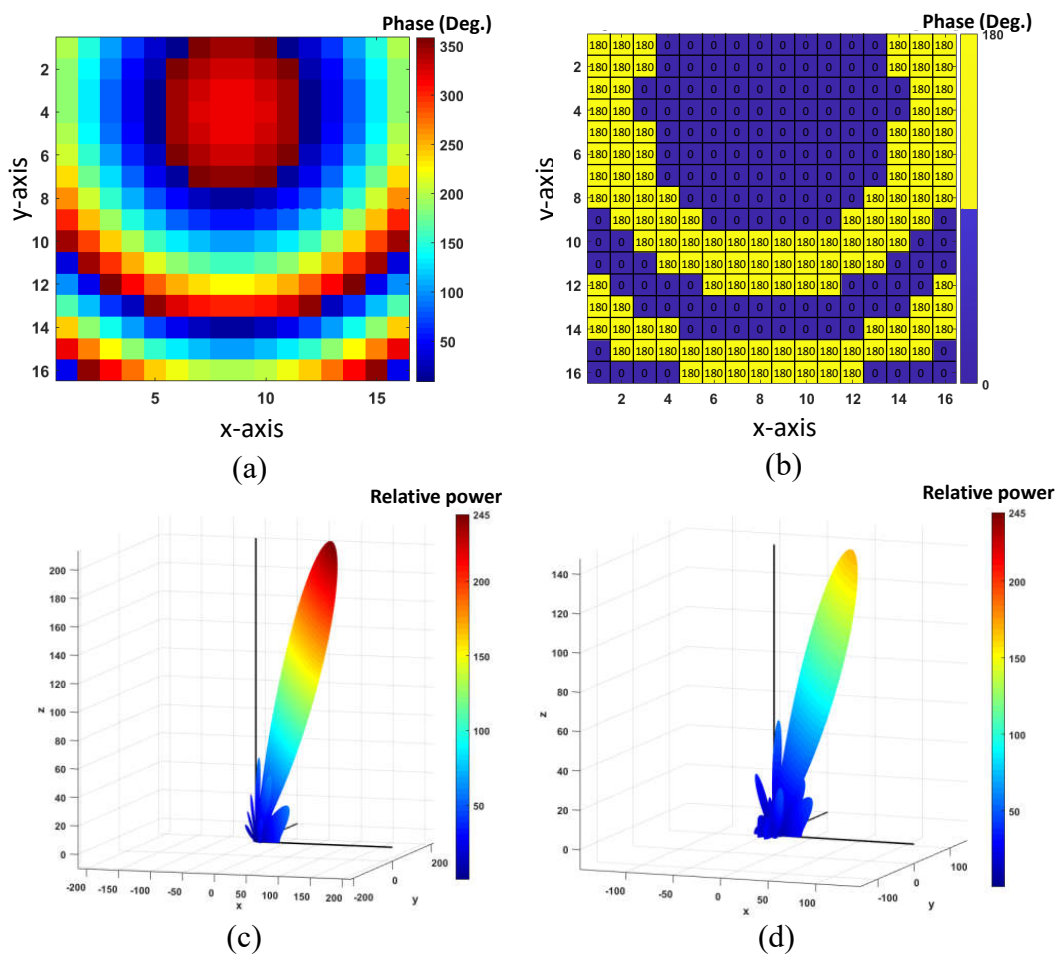


Figure 2. Reflection phase distribution and 3D pattern of the coding metasurface with an electromagnetic (EM) source located at (0 cm, 0 cm, 10 cm) and beam focusing at $(0^\circ, 30^\circ)$: (a) ideal reflection phase distribution; (b) quantized phase distribution; (c) the beam pattern w.r.t ideal phase distribution; (d) the beam pattern w.r.t quantized phase distribution.

2.2. Optimal Phase Control for Adaptive WPT

Due to the imperfection of the manufacturing and experimental setting, the beam may not exactly be directed to the desired direction, which reduces the power received at the receiver. Moreover, in the practical scenarios, the coding metasurface should perform adaptive beam tracking according to the position of the mobile receiving devices. In order to tackle the above-mentioned problem, we propose an optimal phase control scheme allowing us to localize the receiver and focus the power toward that desired position based on the experimental data. The procedure of obtaining the adaptive optimal phase is presented in Figure 3.



Figure 3. The block diagram of the proposed adaptive optimal phase control scheme.

Each unit cell in the metasurface can be considered as an antenna element in an array antenna. Therefore, we can mathematically express the system model as below:

$$y = \sum_{i=1}^M h_i x_i + n, \quad (6)$$

where M is the number of unit cells in the metasurface, n is the additive white Gaussian noise, and h_i is the channel corresponding to the i th unit cell with the state x_i .

For adaptive beam focusing, we have to know the channel to obtain the optimal phase at the metasurface. Analogous to the multiple input single output (MISO) system, we can estimate the channel from each unit cell to the receiver using predefined pilots. Recently, researchers in [23–25] attempted to estimate the channels of the intelligent surface by sending data with one unit cell in “ON” state and the others in “OFF” state at a given training time. However, this method would be impractical, especially when it comes to a huge number of unit cells in the metasurface, as the reflected signal from only one “ON” unit cell is too feeble compared to the rest. Consequently, this leads to unfeasible measurement of the change in the received signal at different training times. Therefore, to tackle this problem, we used 256 independent ON/OFF patterns of the metasurface, which is based on the Hadamard matrix, as training pilots. Then, the adaptive optimal phase control scheme is proposed with the following steps:

- **Training:** sending the signal with 256 independent ON/OFF patterns;
- **Channel estimation:** 256 channels between each unit cell of the metasurface is estimated by multiplying the received signals with the inversion of 256 transmitting patterns;
- **Optimal phase calculation:** optimal phase of each unit cell is obtained by taking the phase of the channel after being conjugated;
- **Phase quantization:** quantizing the phase based on Equation (5);
- **Optimal ON/OFF pattern:** mapping the quantization phases with the ON/OFF state (180° to “ON”, 0° to “OFF”).

3. Design of Coding Metasurface

3.1. Unit Cell Design

In order to have a good performance coding metasurface, a unit cell should be precisely designed to have particular characteristics. As the ISM (industrial, scientific, and medical) band is free and pervasive, we selected 5.8 GHz which is in the ISM band as the target operating frequency in this

work. The final 1-bit unit cell structure is presented in Figure 4. The unit cell is designed on a substrate of Taconic RF-35 with a permittivity of 3.5 and loss tangent of 0.0018. A PIN diode (SMPA1320-079LF-203195B) is integrated with each unit cell to connect the main unit cell with the ground plane through a metal via hole. Thus, it can enable the two states of the unit cell. The operation of the unit cell is ensured by a bias line which is connected to the control board.

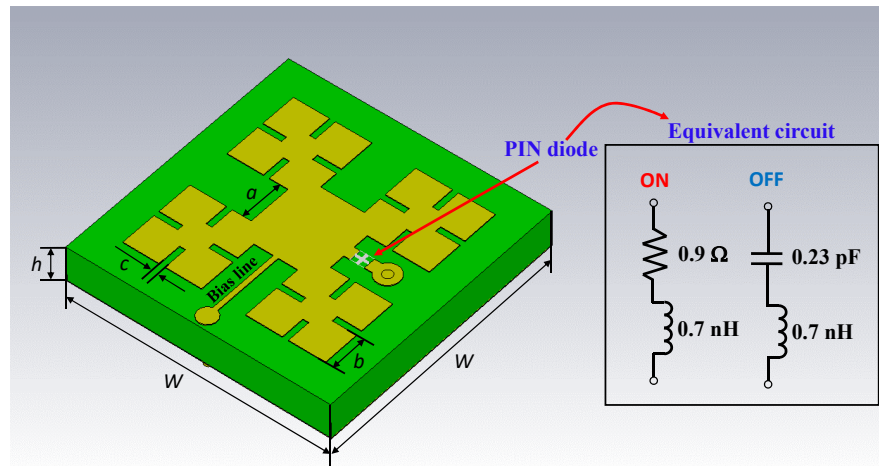


Figure 4. Unit cell structure.

The equivalent circuit for the two states of the PIN diode is given in Figure 4. As can be seen, in an ON state, the PIN diode behaves as a series circuit of a resistance and an inductance, whereas it acts as a series circuit of a capacitance and an inductance. Under an EM wave illumination, the impedance of the PIN diode can be described as:

$$Z_{pin}(\omega) = \begin{cases} R + j\omega L & \text{ON state} \\ j\omega L + \frac{1}{j\omega C} & \text{OFF state.} \end{cases} \quad (7)$$

where $R = 0.9 \Omega$, $L = 0.7 \text{ nH}$, and $C = 0.23 \text{ pF}$. The EM wave will be reflected at the PIN diode and be re-radiated at unit cell surface with the reflection coefficient, which is calculated as:

$$\Gamma(\omega) = \frac{Z_{pin}(\omega) - Z_R}{Z_{pin}(\omega) + Z_R} = |\Gamma|e^{j\phi} \quad (8)$$

where Z_R is the radiation impedance of the unit cell. One should find the structure which provides an appropriate value of Z_R to obtain a 180° phase change between ON and OFF states at the objective frequency. In order to easily figure out the proper value of radiation impedance and reduce the uncontrolled reflection from the unit cell, the unit cell structure should be designed to resonate at the objective frequency. Normally, a rectangular patch with approximately half wavelength dimensions is used as a resonant structure. However, in this work, we used the fractal structure to achieve compact size (a quarter wavelength) but provided the same performance as the rectangular patch. The detailed dimensions of the unit cell are given in the Table 1.

Table 1. The unit cell dimensions.

Parameter	Value (mm)	Parameter	Value (mm)
W	11	h	1.52
a	1.83	b	1.52
c	0.25		

The unit cell is simulated using commercial software CST studio suite and the simulated reflection magnitude and phase of the unit cell are shown in Figure 5. It is obvious that at 5.8 GHz, while the reflection magnitude is almost identical between the ON and OFF state, the reflection phase between the two cases has 180° change. The maximum unit cell loss is around 0.5 dB for the OFF state. It is evident that the proposed 1-bit unit cell is suitable for the coding metasurface. As the phase change between ON/OFF states is relative, we can simply state that a unit cell with an ON state corresponds with a 180° phase reflection and one with an OFF state has a 0° phase reflection.

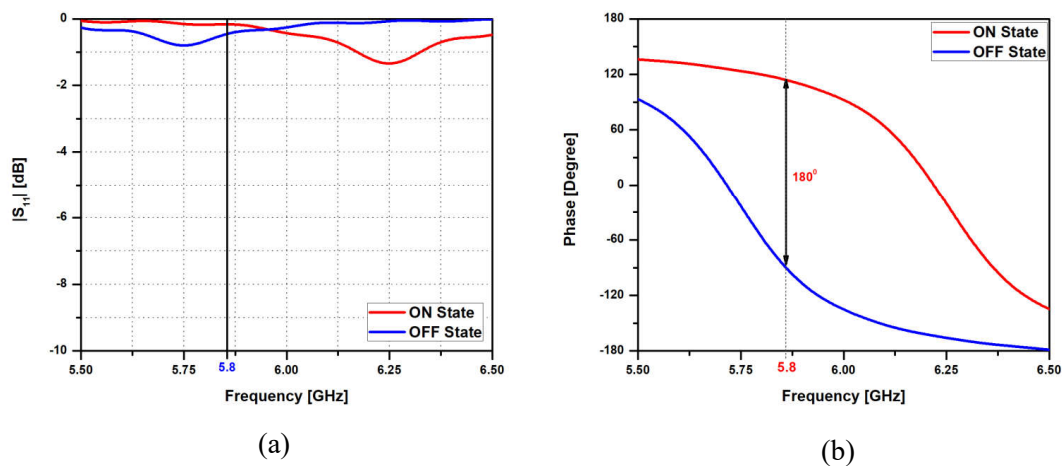


Figure 5. The simulation results of the unit cell: (a) reflection magnitude; (b) reflection phase.

3.2. Coding Metasurface Construction

With the proposed unit cell, a 1-bit 16×16 coding metasurface is constructed and fabricated using printed circuit board technology, as shown in Figure 6. The metasurface has a total size of $176 \text{ mm} \times 176 \text{ mm}$ and is precisely attached to the output pins of the control board as a sandwich structure. To enable the beam focusing ability, the control board plays a crucial role in coding metasurface, which provides an exact voltage to turn the PIN diode in each unit cell ON and OFF. The block diagram and prototype of the control board are presented in Figure 7.

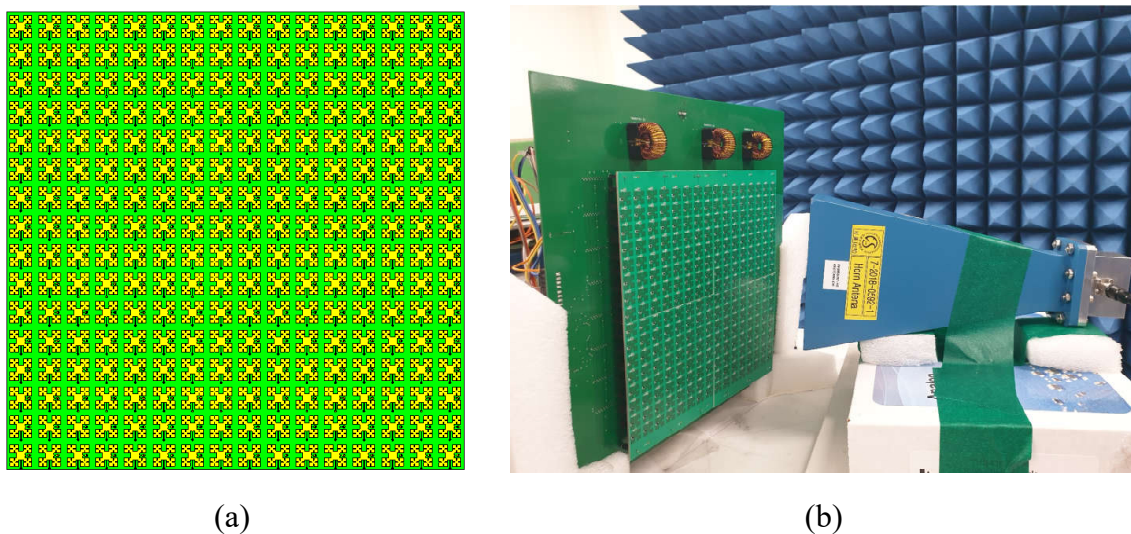


Figure 6. The 1-bit 16×16 coding metasurface model and prototype: (a) metasurface model; (b) experimental set-up.

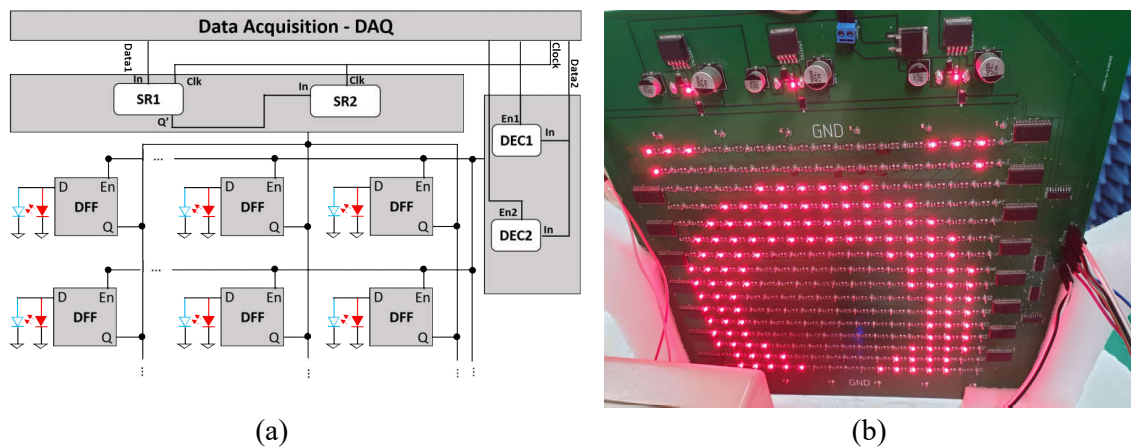


Figure 7. The control board of the coding metasurface: (a) block diagram; (b) the prototype.

As the coding metasurface has 256 unit cells, the control board has to control 256 output pins independently. In order to reduce the complexity of wiring the control board, we used two 8-bit shift registers (SR1 and SR2) to independently set the data for each row. Then, the data will be stored in the D flip flip (DFF), which is enabled by two 3 to 8 line decoders (DEC1 and DEC2). Therefore, by selecting the appropriate row, the data can be independently loaded to the intended row. Consequently, we can control the coding metasurface with any ON/OFF state of the unit cell. The LED is parallel connected to the PIN diode to indicate the state of the unit cell, which gives an observable view of the active ON/OFF pattern of the coding metasurface. All the input data are provided by the data acquisition (DAQ) that is controlled by a LabVIEW program.

4. Results

4.1. Simulation Results

Before fabricating the prototype, a 16×16 coding metasurface is modeled and simulated using CST Studio software to verify the theory. In this simulation, the metasurface is in the XOY plane, and a horn serves as an EM source, which is located at $(-5.7 \text{ cm}, 0 \text{ cm}, 10 \text{ cm})$ or at $(-30^\circ, 0^\circ)$ with respect to the metasurface. Then, an ON/OFF pattern matrix for steering to $(40^\circ, 0^\circ)$ is loaded to the PIN diode of each unit cell. Finally, the simulation results are exported and shown in Figures 8 and 9.

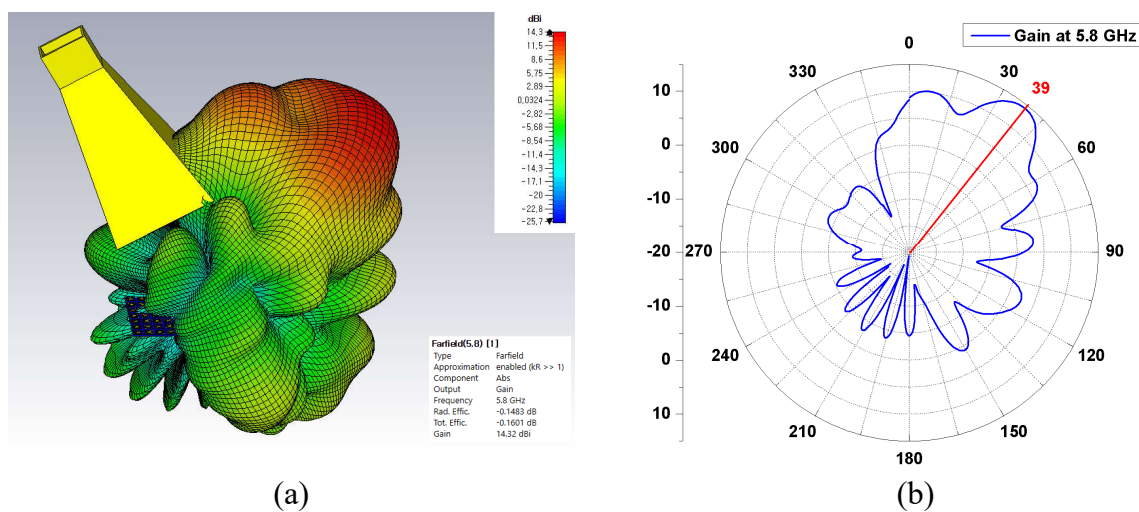


Figure 8. The simulation results: (a) The 3D gain total with the horn and metasurface; (b) the 2D radiation pattern.

It is clearly observed that the coding metasurface is capable of steering the beam to the desired direction with 1° error in the test case. Furthermore, the surface current distribution in Figure 9 is almost coincident with the input ON/OFF coding pattern. Specifically, we can notice that the current distribution of the unit cell in OFF state is considerable compared to the one with the ON state.

As the proposed system transfers the power via EM waves, human exposure and the specific absorption rate (SAR) level should be considered. Figures 10 and 11 present the simulation SAR level (averaged over 1 gram of human tissue) and beam shape when a human head is exposed closely to the metasurface. In this simulation, the metasurface is encoded to focus the beam to $(30^\circ, 0^\circ)$ at the human head, which is placed 50 cm away from the metasurface. The transmitted power is 27 dBm. Figure 10 demonstrates that SAR level at the operating frequency is within the specified limit of 1.6 W/kg regarding to FCC limit. In addition, in the case of human exposure, the beam shape is a bit wider compared to the one without a human head. This results in degrading the gain from 17.3 to around 15 dBi, as shown in Figure 11.

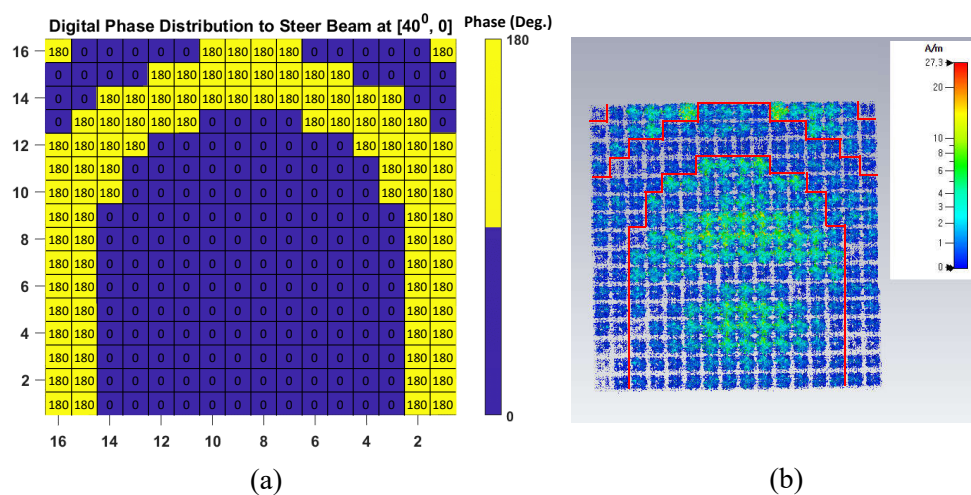


Figure 9. The ON/OFF coding pattern of the coding metasurface: (a) calculated phase distribution matrix; (b) simulated current distribution.

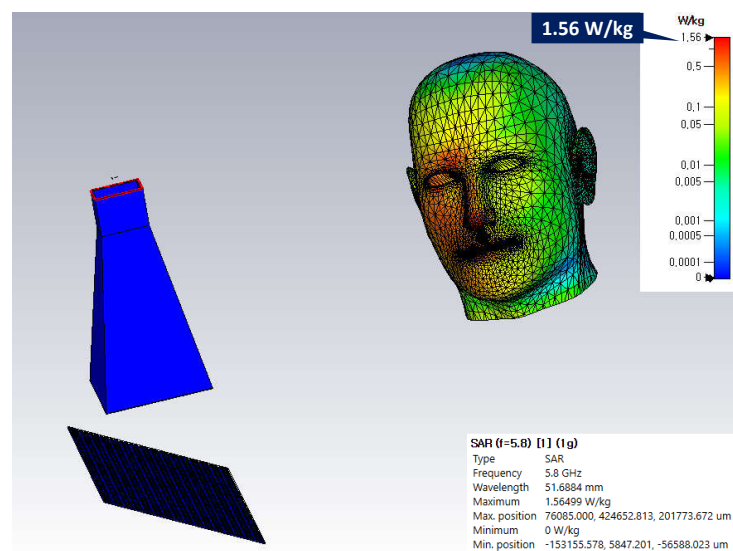


Figure 10. Simulation SAR results with a human head (50 cm away from the metasurface).

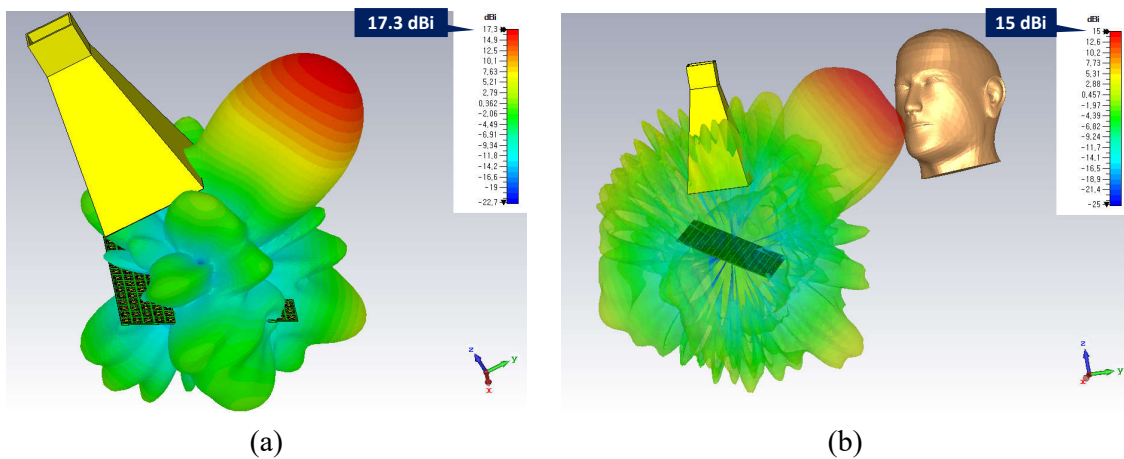


Figure 11. Effect of human exposure in beam shaping: (a) without a human head; (b) with a human head.

4.2. Experimental Results

To demonstrate the capability of the proposed coding metasurface, after fabricating, several tests were done with the prototype.

4.2.1. Beam Steering with Beam Synthesis Scheme

In the first test, we applied ON/OFF coding patterns, which were calculated using the beam synthesis scheme, to verify the beam steering capability of the metasurface. The metasurface is attached to a holder which is perpendicular to the horizontal plane as shown in Figure 7b. A horn antenna working as an EM source is placed at (10 mm, -5.7 mm, 0 mm) with respect to the metasurface to avoid blocking the reflected signal. The measured results are presented in Figure 12.

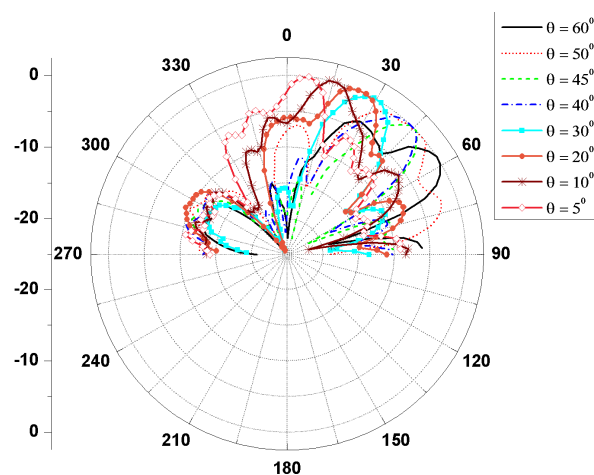


Figure 12. The measured normalized radiation pattern.

We can observe that the coding metasurface can perform beam focusing and steering to a specific direction with the elevation angle (θ) range of 0° to 60° . As a matter of fact, the steerable elevation angle can range from -60° to 60° and the azimuth angle, which the main beam can be focused on, is ($0^\circ, 360^\circ$) by properly assembling the feed horn. However, in the limitation of this paper, we would not demonstrate these results. Further, there are constant errors of about 2° occurred in every cases that may be caused by the imperfection of the experimental setup. Moreover, similar to the theory, the grating lobe appears in the case of steering the beam to 50° and 60° . It is the limitation of the planar metasurface. In addition, the half-power beamwidth (HPBW) ranging from 13° to 27° is likely large

due to the small size of the coding metasurface. A much sharper beamwidth can be attained with a larger coding metasurface.

4.2.2. Adaptive Beam Steering with Optimal Phase Control

To validate the effectiveness of the optimal phase control scheme, firstly, we present the optimal quantized phase distribution and the corresponding beam pattern which is compared to the one from the beam synthesis scheme in Figure 13. It can be observed from Figure 13b that a better beam pattern with a higher transmission coefficient is achieved with optimal phase distribution in comparison with the one of a beam synthesis scheme.

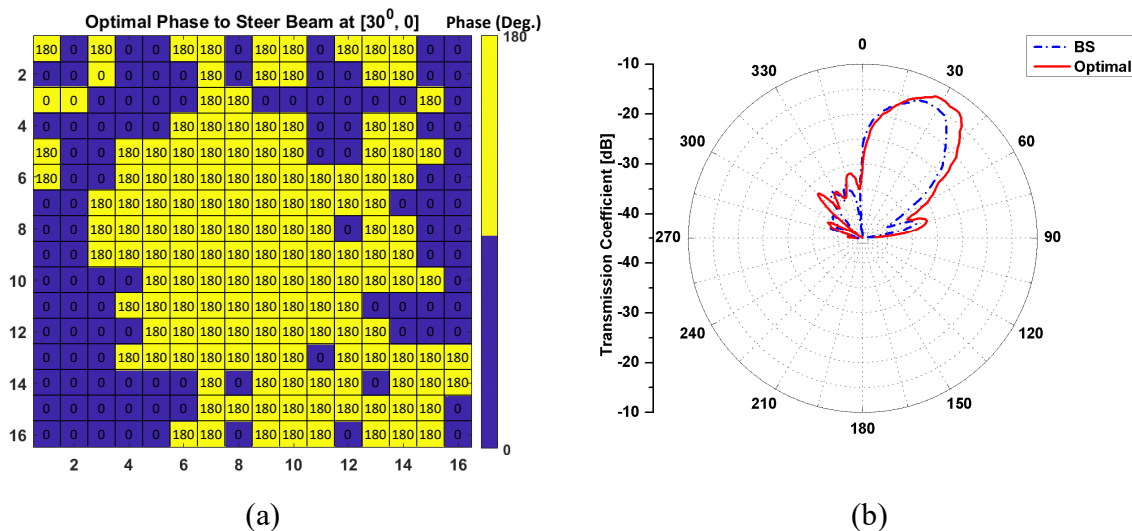


Figure 13. Optimal phase control scheme results: (a) optimal quantized phase distribution for steering beam at $(30^\circ, 0^\circ)$; (b) comparison of beam pattern between optimal phase control (Optimal) and the beam synthesis (BS) schemes.

Furthermore, we measured and compared the efficiency of power transfer between the optimal phase and random phase control schemes in Figure 14a. We also compared the optimal phase control and the beam synthesis schemes in Figure 14b. As can be seen from Figure 14, the proposed scheme demonstrates much higher efficiency in comparison with the random phase control scheme. At the same time, it is clear that the optimal one outperforms the beam synthesis scheme as indicated in Figure 14b. While around 4% efficiency is observed in the optimal phase control scheme at 50 cm with the steering angle of 30° , only around 3% efficiency is achieved in beam synthesis scheme. By extending the size of the coding metasurface, higher power transfer efficiency will be achieved.

The above results were acquired considering only line of sight transmission. However, in actual WPT scenarios, obstacles such as humans and animals might be exposed between the transmitter (Tx) and the receiver (Rx). Hence, this would have a severe effect on power transmission efficiency. To comprehend this problem, we investigated the power transfer efficiency as a human hand and body inserted between Tx and Rx, and the results are indicated in Figure 15. It is evident that the efficiency declines almost 1% with hand blocking and almost drops to 0% with human body blockage.

Actually, we can redo the training to get the optimal phase to enhance the efficiency when the human phantom is inserted. We did re-training with a human body exposed in some positions and compared with the results without re-training as presented in the Table 2. It is clear that remarkable improvement can be achieved by re-training the programmable metasurface when humans are exposed between Tx and Rx.

Table 3 shows the comparison of the proposed system with the previous works. With a fixed beam and large dimensions, the reflect array in [26] provides a higher efficiency compared to the

phased array in [27] and our work. This results not only from the large size of the surface but also from the almost ideal phase distribution used in focusing to a fixed position in this work. This shows the potential of using a metasurface in WPT. The phased array in [27] outperforms our work in transfer distance operating in the lower frequency, which suffers lower loss from transmission path but leads to a physically large system. The performance of our proposed programmable metasurface can be enhanced with a larger size of the metasurface.

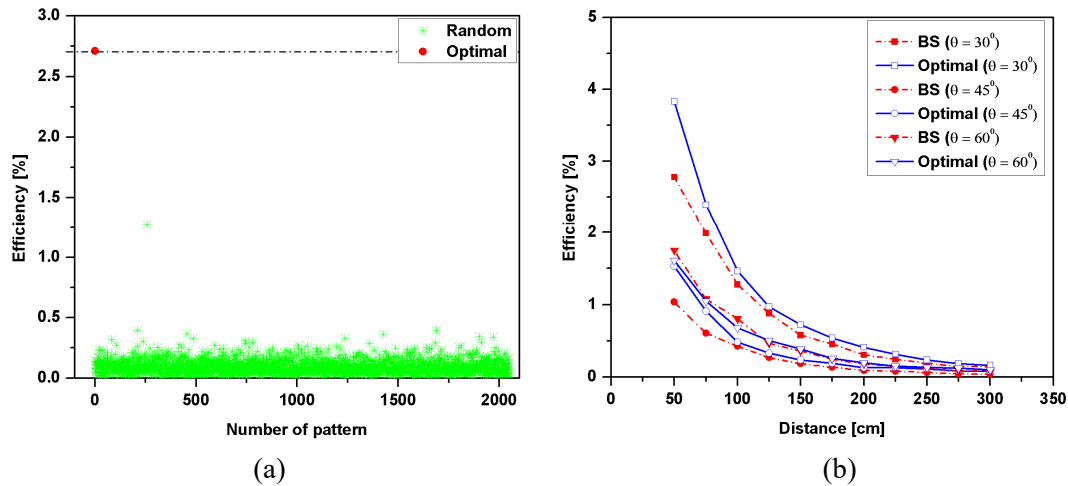


Figure 14. Power transmission efficiency comparison: (a) optimal phase control and random phase control schemes with the steering angle at (30°, 0°); (b) optimal phase control (optimal) and beam synthesis (BS) schemes at different distances.

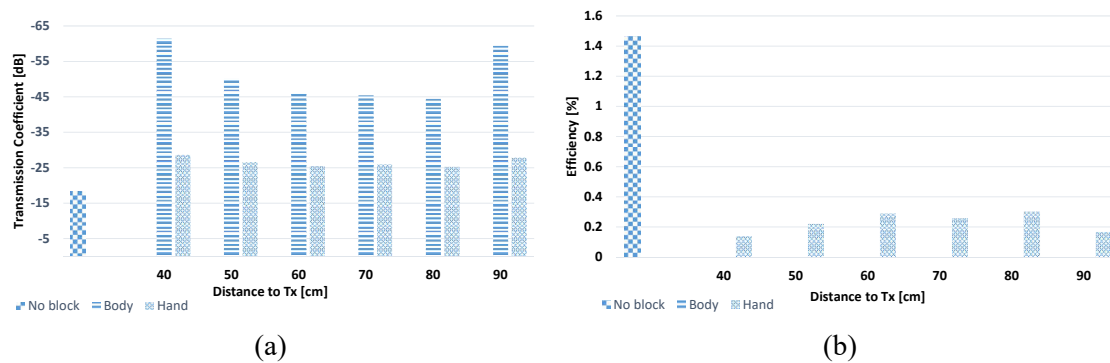


Figure 15. Performance comparison between no block, block with a human body and hand (Rx is 100 cm away from the metasurface (Tx)): (a) transmission coefficient; (b) efficiency.

Table 2. Transmission coefficient enhancement as re-training with human body exposure.

Position	Transmission Coefficient (dB)		Improvement (dB)
	without Re-Training	Re-Training	
1. Close to Tx	−61.4	−54.86	6.54
2. In the middle	−46	−43.83	2.17
3. Close to Rx	−59.4	−54.5	4.9

Table 3. Comparison of the proposed system with previous works.

Reference	Operating Frequency	Dimensions	Method	Adaptability	Distance	Efficiency
[27]	920 MHz	$5.2\lambda \times 2.6\lambda$	Phased array	Yes	6 m	1.2%
[26]	5.8 GHz	$23.59\lambda \times 24.55\lambda$	Reflectarray	No	6 m	25%
Our work	5.8 GHz	$3.4\lambda \times 3.4\lambda$	Coding metasurface	Yes	1 m	1.5%

5. Conclusions

In this paper, a novel 1-bit coding metasurface is proposed and implemented for WPT systems. The coding metasurface is capable of adaptively focusing and steering beam to enhance power transfer efficiency in WPT systems. The proposed metasurface comprises 16×16 compact unit cells which were designed with a fractal structure and an operating frequency of 5.8 GHz. Indeed, both simulations and experiments were conducted to validate the theory. It was demonstrated that the proposed coding metasurface is able to focus the beam to the desired direction with a wide range from -60° to 60° in the elevation angle. For the adaptive beam to be focused on the mobile receiver, the adaptive optimal phase control scheme was proposed and applied. The results prove that the optimal one surpasses the random phase control and beam synthesis schemes. At 50 cm, the coding metasurface with the optimal phase control scheme can provide approximate 4% of power transfer efficiency, while it is just about 3% in the beam synthesis scheme.

Author Contributions: Conceptualization, N.M.T.; Methodology, N.M.T.; Software, N.M.T. and M.M.A.; Validation, N.M.T., M.M.A., J.H.P. and S.I.H.; Formal analysis, N.M.T., M.M.A.; Investigation, N.M.T., M.M.A. and J.H.P.; Resources, J.H.P., S.I.H.; Data curation, N.M.T.; Writing—original draft preparation, N.M.T.; Writing—review & editing, K.W.C. and D.I.K.; Visualization, N.M.T.; Supervision, K.W.C. and D.I.K.; Project administration, K.W.C. and D.I.K. All authors have contributed to the editing and proofreading of this paper.

Funding: This research was supported in part by the National Research Foundation of Korea (NRF) grant funded by the Korean government (MSIP) (2014R1A5A1011478), and in part by the MSIT (Ministry of Science and ICT), Korea, under the ITRC (Information Technology Research Center) support program (IITP-2019-2016-0-00311) supervised by the IITP (Institute for Information & communications Technology Planning & Evaluation).

Conflicts of Interest: The authors declare no conflict of interest.

Abbreviations

The following abbreviations are used in this manuscript:

WPT	Wireless Power Transfer
IoTs	Internet of Things
WSN	Wireless Sensor Network
EM	Electromagnetic
PAA	Phased Array Antennas
HPBW	Half Power Beamwidth
CST	Computer Simulation Technology
FCC	Federal Communications Commission

References

1. Tesla, N. Apparatus for Transmitting Electrical Energy. United States Patent US1119732A, 1 December 1914. Available online: <https://patents.google.com/patent/US1119732A/en> (accessed on 25 November 2019).
2. Xie, L.; Shi, Y.; Hou, T.; Lou, W. Wireless Power Transfer and Applications to Sensor Networks. *IEEE Wirel Commun.* **2013**, *20*, 140–145.
3. Kamalinejad, P.; Mahapatra, C.; Sheng, Z.; Mirabbasi, S.; Leung, V.C.M.; Guan, Y.L. Wireless Energy Harvesting for the Internet of Things. *IEEE Commun. Mag.* **2015**, *53*, 102–108. [CrossRef]
4. Liu, S.; Cui, T.J.; Xu, Q.; Bao, D.; Du, L.; Wan, X.; Tang, W.X.; Ouyang, C.; Zhou, X.Y.; Yuan, H.; et al. Anisotropic coding metamaterials and their powerful manipulation of differently polarized terahertz waves. *Light Sci. Appl.* **2016**, *5*, e16076. [CrossRef] [PubMed]
5. Cui, T.J.; Qi, M.Q.; Zhao, J.; Cheng, Q. Coding metamaterials, digital metamaterials and programmable metamaterials. *Light Sci. Appl.* **2014**, *3*, e218. [CrossRef]
6. Campbell, S.D.; Sell, D.; Jenkins, R.P.; Whiting, E.B.; Fan, J.A.; Werner, D.H. Review of numerical techniques for meta-device desing [Invited]. *Opt. Mater. Express* **2019**, *9*, 1842–1863. [CrossRef]
7. Cui, T.J.; Liu, S.; Zhang, L. Information metamaterials and metasurfaces. *J. Mater. Chem. C* **2017**, *5*, 3644–3668. [CrossRef]

8. Yang, H.; Yang, F.; Xu, S.; Mao, Y.; Li, M.; Cao, X.; Gao, J. A 1-Bit 10×10 Reconfigurable Reflectarray Antenna: Design, Optimization, and Experiment. *IEEE Trans. Antennas Propag.* **2016**, *64*, 2246–2254. [[CrossRef](#)]
9. Yang, H.; Yang, F.; Xu, S.; Li, M.; Cao, X. Experimental Study of a 1-Bit 10×10 Reconfigurable Reflectarray Antenna. In Proceedings of the IEEE International Symposium on Antennas and Propagation & USNC/URSI National Radio Science Meeting, Vancouver, BC, Canada, 19–24 July 2015; pp. 2153–2154.
10. Yang, H.; Yang, F.; Cao, X.; Xu, S.; Cao, J.; Chen, X.; Li, M.; Li, T. A 1600-Element Dual-Frequency Electronically Reconfigurable Reflectarray at X/Ku-Band. *IEEE Trans. Antennas Propag.* **2017**, *65*, 3024–3032. [[CrossRef](#)]
11. Yang, H.; Yang, F.; Xu, S.; Li, M.; Cao, X.; Gao, J. A 1-Bit Multipolarization Reflectarray Element for Reconfigurable Large-Aperture Antennas. *IEEE Antennas Wirel. Propag. Lett.* **2017**, *16*, 581–584. [[CrossRef](#)]
12. Yang, H.; Cao, X.; Yang, F.; Gao, J.; Xu, S.; Li, M.; Chen, X.; Zhao, Y.; Zheng, Y.; Li, S. A programmable metasurface with dynamic polarization, scattering and focusing control. *Sci. Rep.* **2016**. [[CrossRef](#)]
13. Tian, S.; Liu, H.; Li, L. Design of 1-Bit Digital Reconfigurable Reflective Metasurface for Beam-Scanning. *Appl. Sci.* **2017**, *7*, 882. [[CrossRef](#)]
14. Huang, C.; Sun, B.; Pan, W.; Cui, J.; Wu, X.; Luo, X. Dynamical beam manipulation based on 2-bit digitally-controlled coding metasurface. *Sci. Rep.* **2017**, *7*, 42302. [[CrossRef](#)]
15. Li, Y.B.; Li, L.L.; Xu, B.B.; Wu, W.; Wu, R.Y.; Wan, X.; Cheng, Q.; Cui, T.J. Transmission-Type 2-Bit Programmable Metasurface for Single-Sensor and Single-Frequency Microwave Imaging. *Sci. Rep.* **2016**, *6*, 23731. [[CrossRef](#)]
16. Ranaweera, A.L.A.K.; Pham, T.S.; Bui, H.N.; Ngo, V.; Lee, J.W. An active metasurface for field-localizing wireless power transfer using dynamically reconfigurable cavities. *Sci. Rep.* **2019**, *9*, 11735. [[CrossRef](#)]
17. Lang, H.D.; Saris, C.D. Optimization of Wireless Power Transfer Systems Enhanced by Passive Elements and Metasurfaces. *IEEE Trans. Antennas Propag.* **2017**, *65*, 5462–5474. [[CrossRef](#)]
18. Smith, D.R.; Gowda, V.R.; Yurduseven, O.; Larouche, S.; Lipworth, G.; Urzhumov, Y.; Reynolds, M.S. An analysis of beamed wireless power transfer in the Fresnel zone using a dynamic, metasurface aperture. *J. Appl. Phys.* **2017**, *121*, 014901. [[CrossRef](#)]
19. Song, M.; Baryshnikova, K.; Markvart, A.; Belov, P.; Nenasheva, E.; Simovski, C.; Kapitanova, P. Smart table based on a metasurface for wireless power transfer. *Phys. Rev. Appl.* **2019**, *11*, 054046. [[CrossRef](#)]
20. Zhang, P.; Li, L.; Zhang, X.; Liu, H.; Shi, Y. Design, measurement and analysis of near field focusing reflective metasurface for dual-polarization and multi-focus wireless power transfer. *IEEE Access* **2019**, *7*, 110387–110399. [[CrossRef](#)]
21. Yu, S.; Liu, H.; Li, L. Design of near-field focused metasurface for high-efficient wireless power transfer with multifocus characteristics. *IEEE Trans. Ind. Electron.* **2019**, *66*, 3993–4002. [[CrossRef](#)]
22. Li, L.; Liu, H.; Zhang, H.; Xue, W. Efficient wireless power transfer system integrating with metasurface for biological applications. *IEEE Trans. Ind. Electron.* **2018**, *65*, 3230–3239. [[CrossRef](#)]
23. Nadeem, Q.U.A.; Kammoun, A.; Chaaban, A.; Debbah, M.; Alouini, M. S. Intelligent Reflecting Surface Assisted Multi-User MISO Communication. *arXiv* **2019**, arXiv:1906.02360.
24. Yang, Y.; Zheng, B.; Zhang, S.; Zhang, R. Intelligent Reflecting Surface Meets OFDM: Protocol Design and Rate Maximization. *arXiv* **2019**, arXiv:1906.09956.
25. Mishra, D.; Johansson, H. Channel Estimation and Low-Complexity Beamforming Design for Passive Intelligent Surface Assisted MISO Wireless Energy Transfer. In Proceedings of the IEEE International Conference on Acoustics, Speech and Signal Processing (ICASSP), Brighton, UK, 12–17 May 2019; pp. 4659–4663.
26. Lipworth, G.S.; Hagerty, J.A.; Arnitz, D.; Urzhumov, Y.A.; Nash, D.R.; Russell, J. A Large Planar Holographic Reflectarray for Fresnel-Zone Microwave Wireless Power Transfer at 5.8 GHz. In Proceedings of the IEEE/MTT-S International Microwave Symposium-IMS, Philadelphia, PA, USA, 10–15 June 2018; pp. 964–967. [[CrossRef](#)]
27. Aziz, A.A.; Ginting, L.; Setiawan, D.; Park, J.H.; Tran, N.M. Battery-Less Location Tracking for Internet of Things: Simultaneous Wireless Power Transfer and Positioning. *IEEE Internet Things* **2019**, *65*. [[CrossRef](#)]

